Quantitative point source photoacoustic inversion formulas for scattering and absorbing media

Jorge Ripoll*
Institute for Electronic Structure and Laser - Foundation for Research and Technology–Hellas, P.O. Box 1527, 71110 Heraklion, Greece

Vasilis Ntziachristos†
Laboratory for Bio-optics and Molecular Imaging, Center For Molecular Imaging Research, Massachusetts General Hospital & Harvard Medical School, Building 149, 13th Street 5406, Charlestown, Massachusetts 02129-2060, USA
(Received 3 May 2004; revised manuscript received 18 November 2004; published 24 March 2005)

We present here an expression for the photoacoustic contribution of an optical point source in a diffusive and absorbing medium. By using this measurement as a reference, we present a direct inversion formula that recovers the absorption map quantitatively, at the same time accounting for instrumental factors such as the source strength, the shape of the optical pulse, and the impulse response and finite size of the transducers. We further validate this expression through accurate numerical simulations showing that the absorption map is recovered quantitatively in the presence of a rotating geometry. We finally discuss how the presented solutions for point sources within the photoacoustic problem enable the use of concurrent fluorescence and ultrasound measurements as appropriate for a hybrid tomographic system. The proposed system could retrieve absorption information using photoacoustic measurements, and use these data to more accurately describe the fluorescence problem and improve reconstruction fidelity.

DOI: 10.1103/PhysRevE.71.031912 PACS number(s): 87.57.Gg, 42.30.Wb, 42.25.Dd, 42.62.Be

I. INTRODUCTION

Photoacoustic tomography (PAT) has recently demonstrated unprecedented quality in imaging vascular structures deep in small animals [1]. This progress was primarily due to the development of appropriate formulas that can solve for the inverse photoacoustic problem [2,3]. Recent works have clearly shown that the potential of photoacoustic methods is enormous, not only for basic research in tissues and material characterization [4], but also clinically due to its noninvasive nature. Currently, explicit solutions exist for the photoacoustic problem assuming planar illumination [1,2,5]. Deriving expressions for a point source in a scattering and absorbing medium, however, could significantly diversify the potential of the technology in spectroscopic applications, material characterization, and general photoacoustic sensing since no geometrical assumptions of the photon beam and sample are necessary [4]. Furthermore, the use of point sources could lead to quantitative inversion formulas that are independent of the source strength, impulse response, and the finite size of the transducers. This approach is potentially important to tomography where multiangle illumination may have varying strength gains between sources and detectors. Additionally, quantitative inversion formulas are needed if three-dimensional (3D) absorption maps need to be retrieved using PAT, further improving the applicability of PAT *in vivo*.

A particular application derived from obtaining point source solutions would be the creation of a hybrid modality operating on photoacoustic and fluorescence contrast as related to fluorescence molecular tomography (FMT). FMT has recently come into practice for resolving molecular functionality with high specificity deep in tissues [6] based on multiangle fluorescence measurements due to multipoint illumination. While both PAT and FMT modalities will undoubtedly continue to evolve and improve small animal functional and molecular imaging, they also come with highly complementing advantages. Combining these technologies in a hybrid system could yield a modality that employs concurrent measurements of optical and acoustic signals assuming common point illumination sources as is fundamental for improved FMT performance. Such a hybrid approach could allow high-resolution functional measurements achieved by PAT with high molecular sensitivity and specificity achieved by FMT. In addition, PAT images with quantified optical properties could be used as *a priori* information into the FMT inversion problem to significantly improve fluorescence image quality as well. Therefore, solutions of point sources for photoacoustic tomography could also have significant advantages over plane illumination methods [1,5].

We propose here an expression that yields quantitative absorption maps from photoacoustic measurements for a point source in a scattering and absorbing medium that could model arbitrary source distributions in photoacoustic sensing techniques [4]. To achieve this, we present a solution that solves the photoacoustic problem for point sources and arrays of transducers.

This paper is organized as follows. In Sec. II, we present the main equations related to photoacoustics, light propagation in scattering media, and sound propagation to yield the basic equations used in photoacoustic tomography. In Sec. III, we derive the basic expression for a photoacoustic point source in a scattering and absorbing medium, making use of this expression in Sec. IV for the derivation of a direct and quantitative inversion formula. In Sec. V, we present numeri-

*Email address: jripoll@iesl.forth.gr
†Email address: vasilis@helix.mgh.harvard.edu

TABLE I. Symbols, terms, and units used in the derivation of the photoacoustic equations.

Symbol	Term	Units
σ_a	Absorption cross section	cm^2
μ_a	Absorption coefficient	cm^{-1}
μ_s	Scattering coefficient	cm^{-1}
U^{inc}	Incident average intensity	J/cm^2
ρ_m	Mass density	g/cm^3
C	Specific heat	J/g °C
Λ	Thermal conductivity	W/cm °C
E_a	Absorbed energy density	J/cm^3
D_T	Thermal diffusion coeff.	cm^2/s
β	Coefficient of volume thermal expansion (isobaric volume expansion coefficient)	1/°C
v_s	Speed of sound in the medium	cm/s
k	Compressibility	$1/Pa=m^2/Nt$
D	Optical diffusion coefficient	cm
k	Compressibility	$1/Pa=m^2/Nt$

cal experiments where this novel inversion formula is tested, finally presenting our conclusions and future work in Sec. VI.

II. GOVERNING EQUATIONS

In this section, we shall present a summary of the main equations that govern photoacoustic wave generation and propagation, namely (a) the main expressions for the conversion of photon energy density to heat, (b) the equations of light transport in multiple scattering media, and (c) the main expression for acoustic wave propagation.

A. Photoacoustic equations

Let us consider that we have a single absorbing particle of radius a and complex index of refraction n_1 in an infinite homogeneous nonabsorbing medium of real index of refraction n_0. For a given incident optical wavelength λ so that $a \ll \lambda$, the absorption cross section (in cm^2) of this particle is given by [7]

$$\sigma_a = -4\frac{2\pi a}{\lambda}\pi a^2 \,\mathrm{Im}\left\{\frac{n_1 - n_0}{n_1 + 2n_0}\right\}. \tag{1}$$

For a collection of N such particles with no interaction between them and occupying a volume V, the absorption coefficient is given by

$$\mu_a = \rho\sigma_a \tag{2}$$

and has units of cm^{-1}, where $\rho = N/V$ is the particle density. Since the quantities of interest are the average intensity and the energy density, we may define light propagation in this medium in terms of the radiative transfer equation [8,9] for the specific intensity I given in J/m^2 sr. For an incident pulse of light that impinges from a direction $\mathbf{s}$ on this ensemble of particles at a position $\mathbf{r}$, the total absorbed energy E_a per unit volume given in J/cm^3 units is thus defined as [9]

$$E_a(\mathbf{r},t) = \mu_a \int_{4\pi} I(\mathbf{r},t,\hat{\mathbf{s}})d\Omega = \mu_a U^{inc}(\mathbf{r},t), \tag{3}$$

where U^{inc} is the average incident intensity given in J/cm^2. Note that in the constant illumination case (cw), the average intensity is given in W/cm^2 since it is averaged over time. The increase in temperature T at the collection of particles due to the absorbed energy E_a is given by [5]

$$\rho_m C\frac{\partial T(\mathbf{r},t)}{\partial t} - \Lambda\nabla^2 T(\mathbf{r},t) = E_a, \tag{4}$$

where ρ_m is the mass density, C is the specific heat, and Λ is the thermal conductivity (see Table I for units). From Eq. (4), the thermal diffusion coefficient is defined as $D_T = \Lambda/\rho_m C$ in cm^2/s. Typical values of the D_T are in the order of $\sim 1\times 10^{-4}$ cm^2/s for water, compared to $\sim 1\times 10^{9}$ cm^2/s for optical diffusion in tissue. We will neglect thermal diffusion by introducing the following approximation:

$$\Lambda\nabla^2 T(\mathbf{r},t) \ll \rho_m C\frac{\partial T(\mathbf{r},t)}{\partial t}. \tag{5}$$

This validity condition is proven in Ref. [5], where we recall that it is commonly assumed that for time pulses $\tau < 1$ μs, we are well within the limits of approximation Eq. (5). Introducing the approximation Eq. (5) into Eq. (4) and using Eq. (3), we obtain the relationship between the increase in temperature and the absorbed energy,

$$\frac{\partial T(\mathbf{r},t)}{\partial t} \approx \frac{1}{\rho_m C}\mu_a U^{inc}(\mathbf{r},t). \tag{6}$$

Equation (6) forms the basis of photoacoustics, since it relates the absorbed energy with a change in temperature, which will give rise to a change in volume and generate a pressure wave. Equation (6) implies that thermal diffusion can be neglected since typical pulse durations are much shorter than the thermal diffusion time. Once we have de-

fined how an increase of temperature is related to the incident average intensity U^{inc} at a certain point $\mathbf{r}$, we shall now derive the equations that yield the values of U^{inc} inside a scattering and absorbing medium.

B. Light propagation in scattering media

Light propagation in tissue is dominated by absorption due to tissue chromophores such as hemoglobin, and high scattering due to the presence of cellular and subcelluar structures and organelles. A commonly used approximation to model light distribution in tissue is the diffusion approximation [9], by assuming that the average intensity U in Eq. (6) due to an incident energy density S_0 (in units of J/cm^3) follows a diffusion equation,

$$D\nabla^2 U(\mathbf{r},t) - \frac{1}{c}\frac{\partial U(\mathbf{r},t)}{\partial t} - \overline{\mu_a}(\mathbf{r})U(\mathbf{r},t) = -S_0(\mathbf{r},t), \quad (7)$$

where D is the optical diffusion coefficient given in cm units, c is the average speed of light in the medium, and $\overline{\mu_a}(\mathbf{r}) = \mu_a + \Delta\mu_a(\mathbf{r})$ is the spatially dependent absorption in the medium. In the expression for $\overline{\mu_a}(\mathbf{r})$, μ_a is the background absorption as defined in Eq. (2), and $\Delta\mu_a(\mathbf{r}) = \mu_a - \overline{\mu_a}(\mathbf{r})$ is the absorption perturbation. In an infinite homogeneous scattering medium, the general solution in the frequency domain to Eq. (7) is [10]

$$\tilde{U}(\mathbf{r},\omega) = \tilde{U}^{inc}(\mathbf{r}_s,\mathbf{r}) + \frac{1}{4\pi}\int_V \tilde{U}^{inc}(\mathbf{r}_s,\mathbf{r}')\Delta\mu_a(\mathbf{r}') \times g(\kappa_0|\mathbf{r}-\mathbf{r}'|)\mathbf{dr}', \quad (8)$$

where

$$\tilde{U}^{inc}(\mathbf{r}_s,\mathbf{r},\omega) = \frac{1}{4\pi D}\int_V \tilde{S}_0(\mathbf{r}',\omega)g(\kappa_0|\mathbf{r}-\mathbf{r}'|)\mathbf{dr}' \quad (9)$$

is the average intensity due to the incident energy density S_0 in a homogeneous medium for which the 3D Green function g_0 is

$$g(\kappa_0|\mathbf{r}-\mathbf{r}'|) = \frac{\exp(i\kappa_0|\mathbf{r}-\mathbf{r}'|)}{|\mathbf{r}-\mathbf{r}'|}, \quad (10)$$

where

$$\kappa_0 = \sqrt{-\frac{\mu_a}{D} + i\frac{\omega}{cD}} \quad (11)$$

is the frequency-dependent wave number for the optical diffuse photon density wave [11]. By using more complex expressions for the Green function than Eq. (10), complex geometries may be taken into account [12–14]. $U^{inc}(\mathbf{r},t)$ in the time domain is found through Fourier transform as

$$U^{inc}(\mathbf{r},t) = \frac{1}{2\pi}\int_{-\infty}^{+\infty} \tilde{U}^{inc}(\mathbf{r},\omega)\exp(-i\omega t)d\omega. \quad (12)$$

In the following, we shall consider a point source in space and time, and therefore $S_0(\mathbf{r},t) = S_0\delta(\mathbf{r}-\mathbf{r}_s)\delta(t)$, $\tilde{S}_0(\mathbf{r},\omega) = S_0\delta(\mathbf{r}-\mathbf{r}_s)$. In this case, the homogeneous average intensity is given in the frequency domain by

$$\tilde{U}^{inc}(\mathbf{r}_s,\mathbf{r},\omega) = S_0\frac{\exp(i\kappa_0|\mathbf{r}_s-\mathbf{r}|)}{4\pi D|\mathbf{r}_s-\mathbf{r}|} \quad (13)$$

and in the time domain by [15]

$$U^{inc}(\mathbf{r}_s,\mathbf{r},t) = \frac{S_0}{(4\pi Dct)^{3/2}}\exp\left[-\frac{|\mathbf{r}_s-\mathbf{r}|}{4Dct} - \mu_a|\mathbf{r}_s-\mathbf{r}|\right]. \quad (14)$$

Combining Eqs. (14) and (6), we obtain the increase of temperature at a certain position $\mathbf{r}$ due to a point source at $\mathbf{r}_s$. We shall now consider how this increase of temperature is related to the acoustic wave it generates.

C. Sound propagation

As mentioned before, a change in temperature will induce a change in pressure and thus generate an acoustic wave which may be detected by a transducer at a certain distance. To our advantage and considerably simplifying the equations, within fluids the propagating acoustic modes are only longitudinal, the transversal modes existing only in solids. Within fluids, the acoustic generation equations are as follows.

Linear inviscid force equation,

$$\rho_m\frac{\partial^2\mathbf{u}(\mathbf{r},t)}{\partial t^2} = -\nabla p(\mathbf{r},t). \quad (15)$$

Expansion equation,

$$\nabla\cdot\mathbf{u}(\mathbf{r},t) = -\frac{p(\mathbf{r},t)}{\rho_m v_s^2} + \beta T(\mathbf{r},t), \quad (16)$$

where $\mathbf{u}$ is the acoustic displacement, p is the acoustic pressure, ρ_m is the mass density defined before in Eq. (4), β is the isobaric volume expansion coefficient, and v_s is the speed of sound in the medium. Combining Eqs. (15) and (16), we obtain the relationship between the heat source and the pressure produced,

$$\nabla^2 p(\mathbf{r},t) - \frac{1}{v_s^2}\frac{\partial^2 p(\mathbf{r},t)}{\partial t^2} = -\rho_m\beta\frac{\partial^2 T(\mathbf{r},t)}{\partial^2 t}, \quad (17)$$

where the speed of sound is defined as

$$v_s = \frac{1}{\sqrt{\rho_m k}}, \quad (18)$$

where k is the compressibility (see Table I for units). Assuming we have inhomogeneous absorption throughout the medium given by $\overline{\mu_a}(\mathbf{r}) = \mu_a + \Delta\mu_a(\mathbf{r})$ as in Eq. (7), introducing the expression for T given by Eq. (6) into Eq. (17), we obtain

$$\nabla^2 p(\mathbf{r},t) - \frac{1}{v_s^2}\frac{\partial^2 p(\mathbf{r},t)}{\partial t^2} = -\frac{\beta}{C}[\mu_a + \Delta\mu_a(\mathbf{r})]\frac{\partial U(\mathbf{r},t)}{\partial t}. \quad (19)$$

Equation (19) can be expressed in terms of the retarded potential [16] as

$$p(\mathbf{r},t) = p_0(\mathbf{r},t) + \frac{\beta}{4\pi C}\int_V \frac{\mathbf{dr}'}{|\mathbf{r}-\mathbf{r}'|}\Delta\mu_a(\mathbf{r}') \times \left|\frac{\partial U^{inc}(\mathbf{r}',t')}{\partial t'}\right|_{t'=t-(|\mathbf{r}-\mathbf{r}'|/v_s)}, \quad (20)$$

where

$$p_0(\mathbf{r},t) = \frac{\beta\mu_a}{4\pi C}\int_V \frac{\mathbf{dr}'}{|\mathbf{r}-\mathbf{r}'|} \left.\frac{\partial U^{inc}(\mathbf{r}',t')}{\partial t'}\right|_{t'=t-(|\mathbf{r}-\mathbf{r}'|/v_s)} \quad (21)$$

is the homogeneous background pressure wave, and U^{inc} is given by Fourier-transforming Eq. (8). A convenient expression can be reached in the frequency domain for Eq. (20),

$$\tilde{p}(\mathbf{r},\omega) = \tilde{p}_0(\mathbf{r},\omega) - \frac{i\omega\beta}{4\pi C}\int_V \tilde{U}^{inc}(\mathbf{r}',\omega)\Delta\mu_a(\mathbf{r}') \times g(\kappa_a|\mathbf{r}-\mathbf{r}'|)\mathbf{dr}', \quad (22)$$

where

$$\kappa_a = \frac{\omega}{v_s} \quad (23)$$

is the wave number of the acoustic wave, $\tilde{p}(\mathbf{r},\omega) = 1/2\pi\int_{-\infty}^{+\infty} p(\mathbf{r},t)\exp[-i\omega t]dt$, and g is the 3D Green function for the acoustic waves, $g(\kappa_a|\mathbf{r}-\mathbf{r}'|) = \exp(i\kappa_a|\mathbf{r}-\mathbf{r}'|)/|\mathbf{r}-\mathbf{r}'|$.

Once we have defined the equations for photoacoustic source propagation, if quantitative information is to be obtained from Eq. (22), the correct analytical expression of p_0 must be derived, more so in the case of a point source where its contribution to the total pressure may not be distinguished from that of the inhomogeneous background. This is pursued in the following section.

III. PHOTOACOUSTIC POINT SOURCE IN A SCATTERING MEDIUM

In order to obtain the solution at a transducer at a point $\mathbf{r_d}$ due to a point source at $\mathbf{r_s}$ with source strength S_0 in an infinite and homogeneous diffusive medium with absorption coefficient μ_a and diffusion coefficient D, we consider that the Fourier transform of Eq. (21) is given by

$$\tilde{p}_0(\mathbf{r}_s,\mathbf{r}_d,\omega) = -\frac{S_0}{4\pi D}\frac{i\omega\beta\mu_a}{4\pi C}\int_V g(\kappa_0|\mathbf{r}_s-\mathbf{r}'|) \times g(\kappa_a|\mathbf{r}'-\mathbf{r}_d|)\mathbf{dr}'. \quad (24)$$

In order to solve Eq. (24), we shall follow steps similar to those of Ref. [17], where the authors derive the time-dependent expression for a point source in an infinite homogeneous but nondiffusive medium. We would like to emphasize that in the case presented in this work, the methodology used in Ref. [17] may not be applied due to the presence of scattering. Assuming the source is at the origin, by using the spherical symmetry we may convert the 3D wave equation (24) into a 1D wave equation by substitution $P = r\tilde{p}_0$ [10],

$$\frac{\partial^2 P(r,\omega)}{\partial r^2} + \kappa_a^2 = -\frac{i\omega\beta\mu_a}{C}\frac{S_0}{4\pi D}\exp[i\kappa_0 r], \quad (25)$$

in which case the corresponding Green's function is $G = rg = \exp[i\kappa_a r]$. Using this Green function, Eq. (25) may be represented as

$$\tilde{p}_0(r,\omega) = -\frac{i\omega\beta\mu_a}{4\pi C}\frac{S_0}{4\pi D}\frac{1}{r} \times \int_0^\infty \exp[i\kappa_0 r]\exp[i\kappa_a|\mathrm{r}-\mathrm{r}'|]dr. \quad (26)$$

This equation may be analytically solved and yields

$$\tilde{p}_0(\mathbf{r}_s,\mathbf{r}_d,\omega) = -\frac{i\omega\beta\mu_a}{4\pi C}\frac{S_0}{4\pi D|\mathbf{r}_s-\mathbf{r}_d|} \times \left(\frac{2i\kappa_a \exp[i\kappa_0|\mathbf{r}_s-\mathbf{r}_d|]}{\kappa_a^2-\kappa_0^2} + \frac{\exp[i\kappa_a|\mathbf{r}_s-\mathbf{r}_d|]}{i\kappa_a - i\kappa_0}\right), \quad (27)$$

which can be rewritten in terms of $\tilde{U}^{inc}(\mathbf{r}_s,\mathbf{r}_d)$ [see Eq. (13)] as

$$\tilde{p}_0(\mathbf{r}_s,\mathbf{r}_d,\omega) = -\frac{i\omega\beta\mu_a}{4\pi C}\tilde{U}^{inc}(\mathbf{r}_s,\mathbf{r}_d,\omega) \times \left(\frac{2i\kappa_a}{\kappa_a^2-\kappa_0^2} + \frac{\exp[i(\kappa_a-\kappa_0)|\mathbf{r}_s-\mathbf{r}_d|]}{i\kappa_a - i\kappa_0}\right). \quad (28)$$

The time-dependent background pressure due to a point source in an infinite diffusive medium is readily found through inverse Fourier transform of Eq. (28) into the time domain. For convenience, we shall express it as

$$p_0(\mathbf{r}_s,\mathbf{r}_d,t) = \frac{\beta\mu_a}{4\pi C}\frac{\partial f(\mathbf{r}_s,\mathbf{r}_d,t)}{\partial t}.$$

The shape of function f is shown in Fig. 1(a) for typical optical diffusion parameters. As shown, it is *qualitatively* similar to the results reported in Ref. [17], Fig. 1, for the optically nondiffusive case, where only thermal diffusion is considered. There are, however, some distinct differences between the two findings. First, Ref. [17] considers thermal diffusion so that the final time-dependent expression is similar to the f function in Eq. (5), whereas in the optical case it is the time derivative that will yield the photoacoustic pressure. The time derivative of f is shown in Fig. 1(b), where we see that it is approximately a δ function. Therefore, if realistic values of optical pulses are considered through convolution, the qualitative results obtained for the diffusive and nondiffusive medium are equivalent [see Ref [17], Eq. (14)]. This is due to the strongly spatially decaying photoacoustic contribution of the time derivative of a point source, which yields most of the contribution due to the absorption within one mean free path of the source.

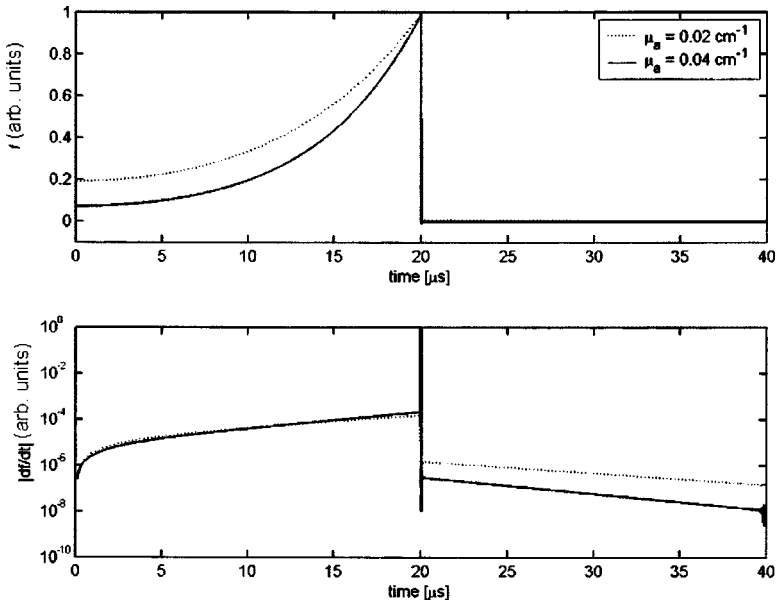

FIG. 1. (a) Normalized value of f vs time in microseconds for $D=0.0333\,\mathrm{cm}, n_0=1.333$, source-detector distance 3 cm, and $\mu_a=0.02\,\mathrm{cm}^{-1}$ (dotted line) and $\mu_a=0.04\,\mathrm{cm}^{-1}$ (solid line). (b) Absolute value of df/dt for the same cases as in (a). Note that $|\mathbf{r}_s-\mathbf{r}_d|/v_s=20\ \mu$s. Acoustical properties used were that of water.

Once the expression for p_0 in Eq. (22) has been found, the direct inversion formulas that yield the spatial map of the inhomogeneous absorption distribution $\overline{\mu_a}(\mathbf{r})=\mu_a+\Delta\mu_a(\mathbf{r})$ can be obtained. The derivation of these formulas is presented in the next section.

IV. INVERSION FORMULAS

The goal of photoacoustic tomography is to obtain the spatial map of the inhomogeneous absorption distribution $\overline{\mu_a}(\mathbf{r})$. Our approach is to retrieve the spatial absorption maps by reconstructing the value of $\Delta\mu_a(\mathbf{r})$ assuming μ_a known. To that end, we followed the robust derivation presented in Ref. [2] for the homogeneous intensity distribution case, and introduced where appropriate the spatial dependence of the incident average intensity U^{inc}. The main difference in this derivation is that we make use of the background pressure wave p_0 as a reference to cancel out all instrumentation-dependent factors (gain, convolution), and take into account the spatially dependent average intensity. An underlying assumption is that of insensitivity to variations of tissue scattering properties, which is based on experimental demonstration of high-quality images, obtained in vivo, even though the scattering variations were not explicitly accounted for [1].

First of all, we will take into account the shape of the optical pulse through convolution with the expression in Eq. (14),

$$u(\mathbf{r}_s,\mathbf{r},t)=H(t-t')^{*}U(\mathbf{r}_s,\mathbf{r},t),$$
$$\tilde{u}(\mathbf{r}_s,\mathbf{r},\omega)=\tilde{H}(\omega)\tilde{U}(\mathbf{r}_s,\mathbf{r},\omega). \tag{29}$$

On the detector side, we will take into account the finite width of the transducers through convolution with a function ρ, and the impulse response of the transducers through function I,

$$P(\mathbf{r}_s,\mathbf{r},t)=I(t-t')^{*}\rho(\mathbf{R}-\mathbf{R}')^{*}p(\mathbf{r}_s,\mathbf{r},t),$$
$$\tilde{P}(\mathbf{r}_s,\mathbf{r},\omega)=\tilde{I}(\omega)\frac{1}{4\pi^2}\int_{-\infty}^{+\infty}\rho(\mathbf{K})\tilde{p}(\mathbf{K},\omega)\exp[-i\mathbf{K}\cdot\mathbf{R}]\mathbf{dK}, \tag{30}$$

where $\mathbf{r}=(\mathbf{R},z)$ are the coordinates in real space, and $\mathbf{k}=(\mathbf{K},q)$ are the corresponding coordinates in Fourier space. In order to follow the derivation used in Ref. [2], where the time dependence is included as a δ function, we shall approximate the incident average intensity as

$$\frac{\partial U^{inc}(\mathbf{r},t)}{\partial t}\simeq\frac{\partial}{\partial t}\left[\left\langle U^{inc}(\mathbf{r},t)\right\rangle\delta(t)\right]=\frac{S_0}{4\pi D}U_0(\mathbf{r})\delta'(t), \tag{31}$$

where $\langle\cdot\rangle$ indicates average over time and

$$U_0(\mathbf{r})=\left.g(\kappa_a|\mathbf{r}_s-\mathbf{r}|)\right|_{\omega=0}=\frac{\exp\left(-\sqrt{\mu_a/D}|\mathbf{r}_s-\mathbf{r}|\right)}{|\mathbf{r}_s-\mathbf{r}|}. \tag{32}$$

Equations (31) and (32) constitute the major approximation included, since we assume that the optical pulse is a δ throughout the volume, whereas from Eq. (14) it is clear that the temporal spread of the intensity is also spatially dependent. Since for realistic volume sizes the temporal spread is on the order of hundreds of nanoseconds, we are well within the limits proposed in Ref. [5]. Including the shape of the optical pulse, Eq. (31) may be expressed as

$$\frac{\partial U^{inc}(\mathbf{r},t)}{\partial t}\simeq-i\omega\frac{S_0}{4\pi D}U_0(\mathbf{r})\frac{1}{2\pi}\int_{-\infty}^{+\infty}\tilde{H}(\omega)\exp(-i\omega t)d\omega. \tag{33}$$

Including expressions (29), (30), and (33) into Eq. (22) and rearranging, we obtain

$$\tilde{P}(\mathbf{r}_s,\mathbf{r}_d)-\tilde{P}_0(\mathbf{r}_s,\mathbf{r}_d)=-\frac{i\omega\beta}{4\pi C}\frac{S_0}{4\pi D}\frac{\tilde{I}(\omega)\tilde{H}(\omega)}{2\pi}\times\int_{-\infty}^{+\infty}dz'\int_{-\infty}^{+\infty}\Phi(\mathbf{r}')^*\rho(\mathbf{R}-\mathbf{R}')\times g(\kappa_a|\mathbf{r}-\mathbf{r}'|)\mathbf{dR}, \quad (34)$$

where we have defined

$$\Phi(\mathbf{r})=\Delta\mu_a(\mathbf{r})U_0(\mathbf{r}) \quad (35)$$

as the variable we want to reconstruct. Fourier transforming the spatial variable $\mathbf{R}$ in both terms in Eq. (34), assuming all detector values are in the same z plane, $z=0$, we obtain [2]

$$\tilde{P}(\mathbf{K},\omega,z=0)-\tilde{P}_0(\mathbf{K},\omega,z=0)=-\frac{i\omega\beta}{4\pi C}\frac{S_0}{4\pi D}\frac{\tilde{I}(\omega)\tilde{H}(\omega)}{2\pi}\frac{1}{4\pi^2}\times\int_{-\infty}^{+\infty}\tilde{\Phi}(\mathbf{K},z')\tilde{\rho}(\mathbf{K})\frac{i}{2\pi q(\mathbf{K})}\exp[iq(\mathbf{K})z']dz', \quad (36)$$

where $q(\mathbf{K})=\mathrm{sgn}(\kappa_a)\sqrt{\kappa_a^2-\mathbf{K}^2}$, sgn( ) being the signum function, and $\tilde{P}(\mathbf{K},\omega,z=0)=1/4\pi^2\int_{-\infty}^{+\infty}\tilde{P}(\mathbf{R},\omega,z=0)\exp[-i\mathbf{K}\cdot\mathbf{R}]\mathbf{dK}$. Rearranging Eq. (36), we obtain

$$\int_{-\infty}^{+\infty}\tilde{\Phi}(\mathbf{K},z')\exp[iq(\mathbf{K})z']dz'=-\frac{2\pi q(\mathbf{K})}{i\tilde{\rho}(\mathbf{K})}\left[\tilde{P}(\mathbf{K},\omega,0)-\tilde{P}_0(\mathbf{K},\omega,0)\right]\times\frac{4\pi C}{i\omega\beta}\frac{S_0}{4\pi D}\frac{8\pi^3}{\tilde{I}(\omega)\tilde{H}(\omega)}. \quad (37)$$

At this point, if we only consider real values of q, i.e., neglect those values for which $\mathbf{K}>\kappa_a$ (evanescent components), the left-hand side of Eq. (37) can be considered a Fourier transform of variable z [2], and therefore

$$\tilde{\Phi}(\mathbf{K},q)=-\frac{2\pi q(\mathbf{K})}{i\tilde{\rho}(\mathbf{K})}\left[\tilde{P}(\mathbf{K},\omega,0)-\tilde{P}_0(\mathbf{K},\omega,0)\right]\times\frac{4\pi C}{i\omega\beta}\frac{S_0}{4\pi D}\frac{8\pi^3}{\tilde{I}(\omega)\tilde{H}(\omega)}. \quad (38)$$

As mentioned before, in order to arrive at expression (38), we have followed Ref. [2]. At this point, by using the fact that $q=\mathrm{sgn}(\omega)\sqrt{(\omega/v_s)^2-\mathbf{K}^2}$, and therefore $\omega=\mathrm{sgn}(q)v_s\sqrt{q^2+\mathbf{K}^2}$, Eq. (38) can be rewritten in terms of $\mathbf{K}$ and q, and the solution is a 3D inverse Fourier transform of $\tilde{\Phi}$. However, since our goal is to obtain quantitative absorption values, we shall divide by the absolute value of the time and spatial Fourier transform of the background pressure wave $|\tilde{P}_0(\mathbf{K},\omega,z=0)|$, thus canceling all convolution factors and constants yielding

$$\tilde{\Phi}(\mathbf{K},q)=\frac{2\pi q(\mathbf{K})}{i}\left(\frac{\tilde{P}(\mathbf{K},q,0)-\tilde{P}_0(\mathbf{K},q,0)}{|\tilde{P}_0(\mathbf{K},q,0)|}\right)\mu_a\times\frac{\mathrm{sgn}(i\omega)}{|\mathbf{r}_s-\mathbf{r}_d|}\left|\frac{2i\kappa_a\exp[i\kappa_0|\mathbf{r}_s-\mathbf{r}_d|]}{\kappa_a^2-\kappa_0^2}+\frac{\exp[i\kappa_a|\mathbf{r}_s-\mathbf{r}_d|]}{i\kappa_a-i\kappa_0}\right|, \quad (39)$$

where $\mathrm{sgn}(i\omega)$ arises from $|i\omega|/i\omega$ and now ω, κ_0, and κ_a need to be rewritten in terms of q as

$$\kappa_0=\mathrm{sgn}(q)\sqrt{-\frac{\mu_a}{D}+i\frac{v_s\sqrt{q^2+\mathbf{K}^2}}{cD}},$$

$$\kappa_a=\mathrm{sgn}(q)\sqrt{q^2+\mathbf{K}^2},$$

$$\omega=\mathrm{sgn}(q)v_s\sqrt{q^2+\mathbf{K}^2}. \quad (40)$$

Once Eq. (39) has been written in terms of $\mathbf{K}$ and q, $\Delta\mu_a(\mathbf{r})$ is found through 3D inverse Fourier transform of $\tilde{\Phi}$ and Eq. (35),

$$\Delta\mu_a(\mathbf{r})=\frac{1}{U_0(\mathbf{r})}\frac{1}{8\pi^3}\int_{-\infty}^{+\infty}\tilde{\Phi}(\mathbf{k})\exp(-i\mathbf{k}\cdot\mathbf{r})\mathbf{dk}, \quad (41)$$

where we recall that $\mathbf{k}=(\mathbf{K},q)$ and $\mathbf{r}=(\mathbf{R},z)$. $\tilde{P}(\mathbf{K},q,z'=0)$ and $\tilde{P}_0(\mathbf{K},q,z'=0)$ are the spatio-temporal Fourier transforms of the total pressure and background homogeneous pressure waves at the XY detector array plane considered as the origin of the z' axis in the reference frame of the source. The derivation of Eq. (41) offers certain advantages over previous developments. First the optical pulse, impulse response, and detector size are inherently deconvolved from the measurements and there is no need to explicitly calculate them or measure them. Second, all constants related to the source strength and other optoacoustical gains are canceled out. This therefore opens the possibility of reconstructing absolute values of the absorption without the need of special calibration schemes, which generally proves to be more accurate in practice for *in vivo* measurements. Finally, this formulation allows for the explicit implementation of point sources with the photoacoustic problem, which enables the simultaneous use of such excitation schemes with fluorescence tomography. We would like to note that if the specific heat C and the isobaric volume expansion coefficient β are spatially dependent and differ from the average values of C and β, what is then retrieved in Eq. (41) is the product $\Delta\mu_a(\mathbf{r})C(\mathbf{r})\beta(\mathbf{r})/\overline{C\beta}$, where $\overline{C}$ and $\overline{\beta}$ represent the average values. The effect of this term, if any, seems to be of small magnitude, given the quality of the reconstructions so far presented in *in vivo* situations [1,18].

We shall now validate Eq. (41) in a numerical simulation in the next section.

V. NUMERICAL SIMULATION

Numerical simulations of Eq. (20) were used for validation of Eq. (41) using realistic experimental parameters. In

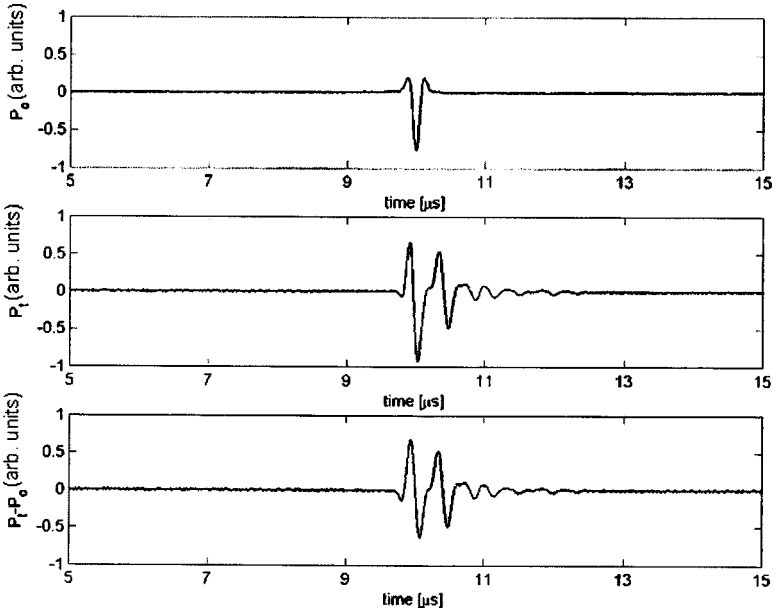

FIG. 2. Example of the acoustic pressure measured for the homogeneous case (P_0), including the absorbing objects (P_t) and the measurement considered in the inversion routine ($P_t - P_0$) for a transducer at $\mathbf{r}_d = (-1.5, 0, 0)$ cm.

order to simulate the measured pressure wave as accurately as possible, we solve numerically Eq. (20) to generate the forward data, including the complete shape of the diffuse light pulse inside the medium, Eq. (14). Rigorous formulation for the photoacoustic wave generated by a hard sphere is available [19], however this derivation is for a nonscattering medium and does not consider optical diffusion. We therefore have opted for solving Eq. (20) numerically. As mentioned before, in the inversion algorithm this pulse is considered a δ throughout the medium, whereas in reality this pulse broadens as it penetrates into tissue. To simulate realistic experimental values, we have considered a temporal spread function for the optical pulse as a Gaussian with full width at half maximum (FWHM) of 10 ns. The impulse response of the transducers is included as a Gaussian with a FWHM of 3 MHz, centered at 3 MHz. Random noise is introduced as 5% of the maximum signal. Finally, a Hanning filter with frequency cut at 6 MHz is used to remove high-frequency noise in Eq. (39). The shapes of the simulated pressure waves are shown in Fig. 2.

The configuration under study is shown in Fig. 3 and consists of a collection of two sets of five objects of diameter 0.05 cm located at $z = [0.25, 0.5, 0.75, 1.0, 1.25]$ cm, with $\mu_a = 0.06\ \mathrm{cm}^{-1}$ those at $x = -0.03$ cm, and $\mu_a = 0.04\ \mathrm{cm}^{-1}$ those at $x = 0.03$ cm, for a background value of $\mu_a = 0.02\ \mathrm{cm}^{-1}$, yielding values of $\Delta\mu_a/\mu_a = 2$ and $\Delta\mu_a/\mu_a = 1$, respectively. In all cases, the acoustical properties considered are those of water, i.e., $\beta = 3.7 \times 10^{-4}/°\mathrm{C}$ at 36 °C and $v_s = 1.5 \times 10^5$ cm/s, and the optical properties are $D = 0.0333$ cm and $n_0 = 1.333$. A point source is located at $\mathbf{r}_s = (0, 0, 0)$ and a line of 128 transducers is located at $x = -1.5$ cm, $y = 0$, with their z positions ranging from 0 to 1.5 cm. The source and the detectors rotate with respect to $\mathbf{r} = (0, 0, 0.75$ cm) with 10 degree steps for a total of 36 rotation angles. The final reconstruction is obtained by averaging the reconstruction obtained at each independent angle. We must stress here that the formulation presented so far corresponds to wide-field transducers; a similar derivation is found for the case of focused transducers, where the main change will be in the expression for the background pressure wave, in which case the contribution will be due to a slice and not to the infinite diffusive volume. Since what we are interested in here is to prove the validity of Eq. (41) for quantitative imaging in the presence of a point source, we shall only consider the case in which objects, source, and detectors are in the same xz plane, assuming wide-field transducers.

Results are shown in Fig. 4, where the normalized case yields approximately the same absorption value for all objects along z (those at $x < 0$ with $\Delta\mu_a/\mu_a = 2$, those at $x > 0$ with $\Delta\mu_a/\mu_a = 1$). In contrast, the direct case which corresponds to using the solution for a point source but not normalizing by the average intensity U_0 as in Eq. (8) has a reduced sensitivity for those objects closer to the center of rotation $\mathbf{r} = (0, 0, 0.75$ cm). Herein, we used a single source for simplicity in presenting the newly developed formulas.

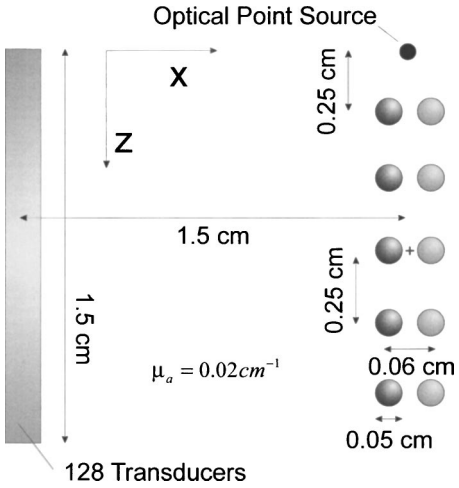

FIG. 3. Geometry used for the numerical simulation where 36 projections at 10° intevals were considered. Center of rotation is marked with a cross.

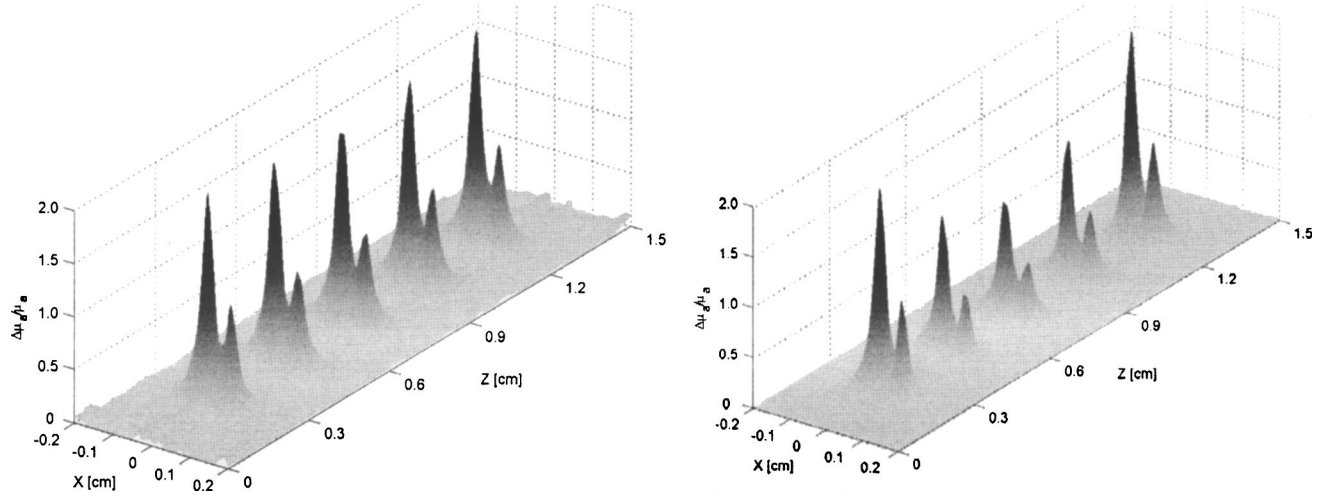

FIG. 4. Results for absorption reconstruction (see text for details), considering 36 projections with 10° increments. Results are shown for the normalized case (left) and the direct case (right) for the normalized reconstructed value $\Delta\mu_a/\mu_a$. Note how the direct case yields different results depending on the radial distance from the center of rotation $r_c=(0,0,0.75\ \mathrm{cm})$.

In order to understand more clearly the effect of normalizing the deconvolved data by the time-averaged intensity, U_0, we plot in Fig. 5 the reconstructed values of Fig. 4 along the $x=-0.3$ and $x=0.3$ lines for the normalized and direct cases. Here the difference between both can be seen more clearly, where, as mentioned before, the sensitivity decays for shorter distances from the center of rotation. In this particular case, we see that the direct method yields a 100% error in the reconstructed value of $\Delta\mu_a/\mu_a$ for the object located at the center of rotation. We would like to emphasize that this error is present whenever the source has a spatially dependent profile and this profile of the incident field is not taken into consideration. In all cases where focused transducers are used and homogeneous intensity can be assumed for each slice, this reconstruction error will of course not be present. A similar approach, however, could be used in these cases in order to connect the absorption maps of each slice by normalizing by the depth-dependent intensity. This approach has been pursued in Refs. [20,21] by analyzing the temporal and spatial profile of the incident beam throughout the volume and including this value in a weighted time-domain delay and sum approach (see Ref. [20] for details).

These simulations demonstrate that quantitative reconstruction of the absorption coefficient is possible with an optical point source. It is interesting to note that multiple sources (of arbitrary gain) may be used to increase the number of tomographic projections yielding improved reconstruction performance for each projection angle. While conventional photoacoustic tomography does not lack in image quality when using planar illumination, the methodology developed herein is optimally suited for concurrent photoacoustic and fluorescence tomographic measurements as appropriate for a hybrid system.

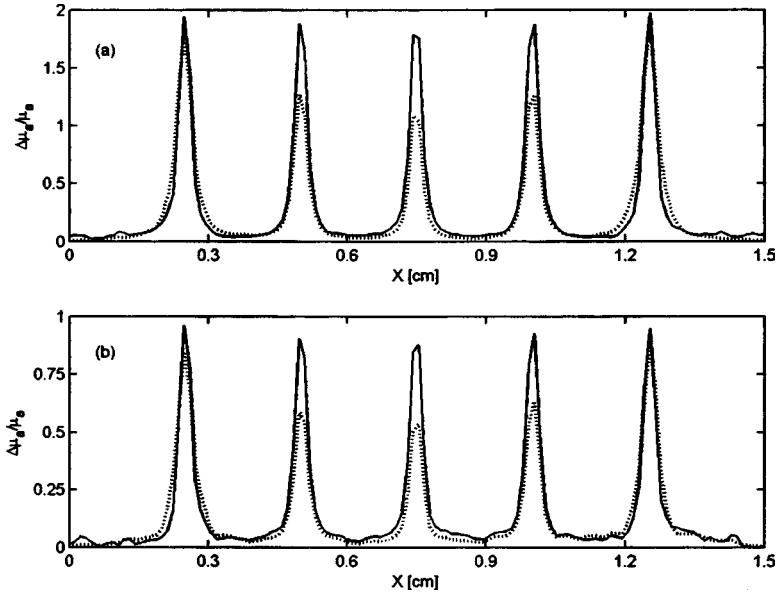

FIG. 5. Slice of the reconstructions obtained in Fig. 3 through the $\mu_a=0.06\ \mathrm{cm}^{-1}, \Delta\mu_a/\mu_a=2$ (top) at $x=-0.03$ cm, and $\mu_a=0.04\ \mathrm{cm}^{-1}, \Delta\mu_a/\mu_a=1$ (bottom) at $x=0.03$ cm. Solid lines, normalized solution; dotted lines, direct solution.

VI. CONCLUSIONS

In conclusion, we have developed an expression for the pressure wave generated by an optical point source in an infinite diffusive and absorbing medium. We have shown that by using this background pressure wave, the composite measurements collected are inherently deconvolved of the instrument transfer function and that instrumentation-dependent factors such as the source strength and optical and acoustical constants cancel out, simplifying experimental practices. By making use of the expression for a point source, the implementation of arbitrary source distributions in photoacoustic sensing techniques is straightforward. Finally, we have presented an expression that accounts for the spatial dependence of the incident optical intensity, thus opening the possibility of performing quantitative absorption photoacoustic tomography with point sources such as optical fibers. The approach presented is independent of source strength, since gain terms cancel out, which makes possible the inclusion of the optical source as another parameter to probe the inhomogeneous medium. This opens the possibility of obtaining 3D spatial absorption distributions in tissues with quantitative functional information based on spectral decomposition of photoacoustic measurements.

Apart from the above-mentioned advantages in photoacoustic-related techniques, this new methodology bridges photoacoustic and fluorescence molecular tomography inversion technology and instrumentation. FMT and other optical tomography modalities currently used to image tissue make use of multiple point-source positions in order to generate different projections mainly due to light scattering in tissue, these techiques are usually not efficient using plane-wave illumination. The formulation presented here enables a system where photonic and photoacoustic measurements are simultaneously obtained using the same photon source for fluorescence excitation and photoacoustic pressure wave generation. Such a combination offers the possibility of feeding the PAT information into the FMT inversion to yield superior quality and information content measurements. A combined system could exceed the performance of a standard multimodality approach allowing for a true hybrid method which yields images of superior information and quality compared to images provided by these systems operated independently. This technology could potentially enable highly accurate, specific, and quantitative investigations of gene expression and molecular function in small animals and possibly humans.

ACKNOWLEDGMENTS

This work was supported in part by National Institutes of Health Grants No. ROI EB000750-1 and No. R33-CA91807 and NASA/NCI Contract No. BAA-NO1-CO-17016-32. J.R. acknowledges support from E.U. Integrated Project "Molecular Imaging" LSHG-CT-2003-503259 and E.U. STREP "TRANS-REG" LSHG-CT-2004-502950.

[1] X. Wang *et al.*, Nat. Biotechnol. **21**, 803 (2003).
[2] Y. Xu, D. Feng, and L. H. Wang, IEEE Trans. Med. Imaging **21**, 823 (2002).
[3] Y. Xu and L. H. Wang, Phys. Rev. Lett. **92**, 033902 (2004).
[4] A. C. Tam, Rev. Mod. Phys. **58**, 381 (1986).
[5] R. A. Kruger *et al.*, Med. Phys. **22**, 1605 (1995).
[6] V. Ntziachristos *et al.*, Nat. Med. **8**, 757 (2002).
[7] H. C. van de Hulst, *Light Scattering by Small Particles* (Dover Publ., New York, 1981).
[8] S. Chandrasekhar, *Radiative Transfer* (Dover, New York, 1960).
[9] A. Ishimaru, *Wave Propagation and Scattering in Random Media* (Academic, New York, 1978).
[10] G. B. Arfken and H. J. Weber, *Mathematical Methods for Physicists* (Academic Press, New York, 1995).
[11] D. A. Boas *et al.*, Phys. Rev. E **47**, R2999 (1993).
[12] J. Ripoll and M. Nieto-Vesperinas, J. Opt. Soc. Am. A **16**, 1453 (1999).
[13] J. Ripoll *et al.*, Phys. Rev. E **64**, 051917 (2001).
[14] J. Ripoll and V. Ntziachristos, J. Opt. Soc. Am. A **20**, 1103 (2003).
[15] M. S. Patterson, B. Chance, and B. C. Wilson, Appl. Opt. **28**, 2331 (1989).
[16] J. A. Stratton, *Electromagnetic Theory* (McGraw-Hill, New York, 1941).
[17] I. G. Calasso, W. Craig, and G. J. Diebold, Phys. Rev. Lett. **86**, 3550 (2001).
[18] X. Wang *et al.*, Opt. Lett. **29**, 730 (2004).
[19] G. J. Diebold, A. C. Beveridge, and T. J. Hamilton, J. Acoust. Soc. Am. **112**, 1780 (2002).
[20] C. G. A. Hoelen and F. F. M. de Mul, Appl. Opt. **39**, 5872 (2000).
[21] C. G. A. Hoelen *et al.*, Opt. Lett. **23**, 648 (1998).